New Phytologist

The PRT6 N-degron pathway restricts VERNALIZATION 2 to endogenous hypoxic niches to modulate plant development

Journal:	*New Phytologist*
Manuscript ID	NPH-MS-2019-31341.R2
Manuscript Type:	MS - Regular Manuscript
Date Submitted by the Author:	03-Feb-2020
Complete List of Authors:	Labandera, Anne-Marie; University of Birmingham, School of Biosciences Tedds, Hannah; University of Birmingham, School of Biosciences Bailey, Mark; University of Birmingham, School of Biosciences Sprigg, Colleen; University of Birmingham, School of Biosciences Etherington, Ross; University of Birmingham, School of Biosciences Akintewe, Olunwatunmise; University of Birmingham, School of Biosciences Kalleechurn, Geetika; University of Birmingham, School of Biosciences Holdsworth, Michael; University of Nottingham, School of Biosciences; Gibbs, Daniel; University of Birmingham, School of Biosciences; University of Birmingham, School of Biosciences
Key Words:	flowering time, hypoxia, N-degron pathway, polycomb, PRC2, proteolysis, root, vernalization

The PRT6 N-degron pathway restricts VERNALIZATION 2 to endogenous hypoxic niches to modulate plant development

Anne-Marie Labandera[1], Hannah M. Tedds[1], Mark Bailey[1], Colleen Sprigg[1], Ross D. Etherington[1], Olunwatunmise Akintewe[1], Geetika Kalleechurn[1], Michael J. Holdsworth[2] and Daniel J. Gibbs[1*]

[1] School of Biosciences, University of Birmingham, Edgbaston, B15 2TT, UK

[2]School of Biosciences, University of Nottingham, Loughborough, LE12 5RD, UK

[*]Correspondence: Daniel J. Gibbs (d.gibbs@bham.ac.uk) (+44(0)121454309)

Total word count: 6618

Introduction: 1359

Materials and Methods: 984

Results: 2826

Discussion: 1449

Main Figures: 6 (all in colour)

Supplemental Tables: 1

Supplemental Figures: 1

Summary

- VERNALIZATION2 (VRN2), an angiosperm-specific subunit of the polycomb repressive complex 2 (PRC2), is an oxygen (O_2) regulated target of the PCO branch of the PRT6 N-degron pathway of ubiquitin-mediated proteolysis. How this post-translational regulation coordinates VRN2 activity remains to be fully established.
- Here we use *Arabidopsis thaliana* ecotypes, mutants and transgenic lines to determine how control of VRN2 stability contributes to its functions during plant development.
- VRN2 localises to endogenous hypoxic regions in aerial and root tissues. In the shoot apex, VRN2 differentially modulates flowering time dependent on photoperiod, whilst its presence in lateral root primordia and the root apical meristem negatively regulates root system architecture. Ectopic accumulation of VRN2 does not enhance its effects on flowering, but does potentiate its repressive effects on root growth. In late-flowering vernalization-dependent ecotypes, VRN2 is only active outside meristems when its proteolysis is inhibited in response to cold exposure, since its function requires concomitant cold-triggered increases in other PRC2 subunits and co-factors.
- We conclude that the O_2-sensitive N-degron of VRN2 has a dual function, confining VRN2 to meristems and primordia, where it has specific developmental roles, whilst also permitting broad accumulation outside of meristems in response to environmental cues, leading to other functions.

Keywords

Flowering time, hypoxia, N-degron pathway, polycomb, PRC2, proteolysis, root, vernalization, VIN3

Introduction

Plants need to accurately regulate gene expression to appropriately co-ordinate their development in response to changing environmental conditions. Such regulation occurs at the direct transcriptional level, through the action of transcription factors, but also epigenetically through a combination of DNA methylation and modification of histone tails in the nucleosomes that make up chromatin. One of the best characterised histone modifying enzymes in eukaryotes is the polycomb respressive complex 2 (PRC2), a multisubunit holoenzyme that catalyses the deposition of the Histone H3 lysine 27 trimethylation (H3K27me3) mark on chromatin (Simon & Kingston, 2009; Margueron & Reinberg, 2011). H3K27me3 promotes compaction of nucleosomes, and therefore acts as a repressor of transcription through switching off gene expression by limiting transcription factor occupancy. The canonical PRC2 comprises four core subunits, and several of these have expanded in number in plants, indicating enhanced flexibility in the composition and activity of individual PRC2s (Hennig & Derkacheva, 2009; Mozgova *et al.*, 2015). PRC2 complexes in *Arabidopsis thaliana* (hereafter Arabidopsis) are named according to which of three homologs of the *Drosophila melanogaster* SUPPRESSOR OF ZESTE 12 (Su(z)12) subunit they recruit: FERTILIZATION INDEPENDENT 2 (FIS2), EMBRYONIC FLOWERING 2 (EMF2) and VERNALIZATION 2 (VRN2). Both EMF2 and VRN2 are expressed in sporophytic tissues, where they form PRC2 complexes in association with the methlytransferases CURLY LEAF (CLF) or SWINGER (SWN). CLF and SWN can act interchangeably with EMF2 and VRN2 to regulate overlapping and distinct functions, particularly in the control of shoot development and flowering (Gendall *et al.*, 2001; Yoshida *et al.*, 2001). In contrast, the expression and activity of FIS2 and its cognate methyltransferase MEDEA (MED) are exclusive to the gametophyte, where FIS2-PRC2 prevents fertilization in the absence of pollination (Yadegari *et al.*, 2000). Common to all three PRC2 complexes is FERTILIZATION INDEPENDENT ENDOSPERM (FIE), a homolog of Drosophila EXTRA SEX COMBS, and the only component in Arabidopsis that is not encoded by multiple family members (Ohad *et al.*, 1999).

VRN2 was first identified as a major regulator of the vernalization response in *Arabidopsis* ecotypes that require prolonged winter to initiate flowering in spring (Chandler *et al.*, 1996; Sheldon *et al.*, 2000; Gendall *et al.*, 2001). During cold

exposure, VRN2-PRC2 accumulates, and through associations with other cold-specific accessory proteins – including the PHD protein VERNALIZATION INSENSTITIVE3 (VIN3) and its homolog VRN5 – it contributes to histone methylation and epigenetic repression of the floral inhibitor gene *FLOWERING LOCUS C (FLC)* (Sung & Amasino, 2004; Wood *et al.*, 2006; Greb *et al.*, 2007; Costa & Dean, 2019). PRC2-mediated *FLC* silencing occurs in distinct phases; initial methylation at a nucleation site in the cold requires VRN2-PRC2 in association with SWN, whilst subsequent H3K27me3 spreading throughout the *FLC* gene body occurs in the warmth and is dependent on PRC2-CLF (Yang *et al.*, 2017; Costa & Dean, 2019). Mutations of VRN2 and VRN2-like proteins in Arabidopsis, rice and *Medicago truncatula* (Medicago) also lead to non-vernalization associated flowering phenotypes, indicating additional roles for VRN2 in autonomous flowering pathways (Gendall *et al.*, 2001; Yang *et al.*, 2013; Jaudal *et al.*, 2016). Further to its role in vernalization, VRN2 has been implicated in the control of seed dormancy (Auge *et al.*, 2017), seed development (Roszak & Kohler, 2011), vascular patterning and root cell proliferation (de Lucas *et al.*, 2016), somatic cell de-differentiation (Ikeuchi *et al.*, 2015), and hypoxia and submergence tolerance (Gibbs *et al.*, 2018).

Although many functions and targets of plant PRC2s are known, direct mechanisms controlling their activity, composition, and specificity are less well established. Spatiotemporal differences in the expression of SWN, CLF, EMF2 and VRN2 have been demonstrated in specific root cell types, indicating that the patterning of their expression contributes to their diverse functions (de Lucas *et al.*, 2016). However, discrepancies in promoter activity, mRNA abundance, and protein accumulation indicate that PRC2 subunits are also under post-translational control (Wood *et al.*, 2006; de Lucas *et al.*, 2016). We previously identified VRN2 as an oxygen (O_2)-regulated target of the PCO branch of the PRT6 N-degron pathway of proteolysis via its conserved Met-Cys-initiating N-terminus, and showed that it positively regulates hypoxia tolerance (Gibbs *et al.*, 2018). VRN2 was co-opted to this regulatory pathway in flowering plants, following duplication and N-terminal truncation of an EMF2-like ancestor that contained a latent internal N-degron (Chen *et al.*, 2009; Gibbs *et al.*, 2018). Posttranslational control of VRN2 limits its accumulation in the absence of environmental stimuli that inhibit its proteolysis, including low-O_2 (hypoxia) and long-term exposure to cold temperatures (Gibbs *et al.*, 2018). How this regulation of VRN2

stability contributes to its known and undescribed functions during development remains to be determined.

Hypoxia in plants occurs frequently due to O_2 diffusion limitation, rapid consumption rates in tissues with high energy demands, and in response to flooding stress (Bailey-Serres *et al.*, 2012; van Dongen & Licausi, 2015; Considine *et al.*, 2017). In plants, the transcriptional response to hypoxia is coordinated by ERFVII transcription factors, which are O_2 and nitric oxide (NO) labile targets of the PRT6 N-degron pathway (Gibbs *et al.*, 2011; Licausi *et al.*, 2011; Gibbs *et al.*, 2014a; Gibbs *et al.*, 2015). In O_2-replete conditions, ERFVIIs undergo a series of N-terminal modifications, including methionine excision, cysteine oxidation and N-terminal arginylation, which promotes their degradation by the N-recognin E3 ligase PROTEOLYSIS6 (PRT6) (Gibbs *et al.*, 2014b; Weits *et al.*, 2014; Gibbs *et al.*, 2016; White *et al.*, 2017). Enhanced stabilisation of ERFVIIs prior to and during hypoxia is critical for survival of low-O_2 (Gibbs *et al.*, 2011; Licausi *et al.*, 2011; Schmidt *et al.*, 2018; Dissmeyer, 2019; Hartman *et al.*, 2019; Holdsworth *et al.*, 2019; Lin *et al.*, 2019). Furthermore, control of ERFVII stability also regulates responses to other abiotic stresses and pathogen attack (de Marchi *et al.*, 2016; Vicente *et al.*, 2017; Vicente *et al.*, 2019).

In addition to flooding induced O_2 deprivation, endogenous hypoxic niches occur naturally in certain plant tissues, where they play a necessary and positive role in regulating development (Borisjuk & Rolletschek, 2009; Kelliher & Walbot, 2012; Meitha *et al.*, 2015; Considine *et al.*, 2017; Meitha *et al.*, 2018). For example, a conserved hypoxic niche in the shoot apical meristem (SAM) coordinates leaf development by constraining the accumulation of the locally expressed transcriptional regulator LITTLE ZIPPER 2 (ZPR2), a Cys-initiating N-degron pathway target that controls primordia formation through repressing the activity of HD-ZIP III regulators (Weits *et al.*, 2019). A hypoxic niche is also established in lateral root primordia (LRP), triggering ERFVII stabilisation to attenuate auxin signalling by inhibiting LRP developmental genes (Shukla *et al.*, 2019). Furthermore, ERFVIIs coordinate early seedling establishment during the skoto- to photo-morphogenic transition, sensing O_2 availability to regulate apical hook opening and limit the production of harmful chlorophyll precursors before light is perceived (Abbas *et al.*, 2015; Zhang *et al.*, 2018). Thus, in addition to having a general role in coordinating hypoxia stress

155 survival, ERFVIIs also have separate context- and tissue-specific developmental
156 functions.

157 Here we investigate how regulation of VRN2 through its O_2-sensitive N-degron
158 controls its spatiotemporal accumulation and function during development in
159 *Arabidopsis*. Under non-stressed and ambient growth conditions, VRN2 protein is
160 largely confined to regions of the plant that are characterised by hypoxic niches,
161 namely the SAM and young leaf primordia (hereafter, the shoot apex) and LRPs, as
162 well as primary and lateral root meristematic zones. Localisation of VRN2 to the shoot
163 apex modulates the photoperiod-dependent transition to reproductive growth,
164 independently of its role in vernalization pathways, whilst its accumulation in discrete
165 regions of the root negatively regulates root system architecture by limiting root
166 branching and primary root growth. Moreover, we show that ectopic stabilisation of
167 VRN2 through genetic manipulation is insufficient to trigger the vernalization response
168 in the absence of cold exposure, since increases in other PRC2 components and cold-
169 specific factors are also required for appropriate silencing of *FLC* to induce flowering
170 in response to winter. We conclude that the N-degron of VRN2 is necessary for
171 preventing ectopic accumulation outside of meristems and primordia, where it has
172 specific roles in regulating growth and development. In contrast, under certain
173 environmental conditions, including cold exposure and hypoxia, proteolysis is inhibited
174 and VRN2 accumulates throughout the plant where along with other context-specific
175 factors it adopts a different set of developmental functions.

176

177 **Materials and Methods**

178

179 **Plant growth and materials**

180 *Arabidopsis thaliana* (L.) Heynh lines were obtained from the Arabidopsis Stock Centre
181 (NASC), except for: Col-0 FRI-Sf2 (Lee *et al.*, 1994), from Dr. Jie Song, Imperial
182 College London, UK; *pVRN2::VRN2-FLAG* and *vrn2-1 fca-1* (Wood et al., 2006), from
183 Dr. Chris Helliwell, CSIRO, Australia; *pFLC::FLC-GUS* (Sheldon *et al.*, 2008), from Dr.
184 Candice Sheldon, CSIRO, Australia. The WT and Cys2Ala *pVRN2::VRN2-GUS*
185 transgenics in Col-0 and *prt6-1*, as well as *vrn2-5*, *prt6-1*, and *prt6-1 vrn2*-5 lines were
186 described previously (Gibbs *et al.*, 2018). Mutant combinations were generated by

crossing, and full knockouts confirmed by PCR and RT-PCR (primers in Table S1). Typically, seeds were surfaced sterilized in 20% Parazone, plated on half-strength Murashige and Skoog (1/2 MS) medium (1% agar, pH 5.7), and stratified at 4°C for a minimum of 2 days, before being transferred to long day (LD; 16hL:8hD) conditions under white fluorescent light (90–100 μmol m^{-2} s^{-1}) at 22°C, and transferred to soil after two weeks.

Plant phenotypic analyses

For flowering time assessment, seedlings were grown on vertical 1/2 MS plates for 7 days, before being transferred to soil under LD or short day (SD; 8hL:16hD, 22°C) conditions. Flowering time was determined by counting the number of rosette leaves and day number at bolting. For vernalization experiments, following an initial 7 days growth at 22°C, plates were transferred to SD at 5°C for the appropriate number of weeks. For non-vernalized controls, 1 week at 5°C was correlated with 1 day growth at 22°C. Following these treatments, seedlings were harvested for protein/RNA extraction, or transferred to soil and grown under LD at 22°C until bolting, at which point rosette leaf number and day number was counted. For root assays, seedlings were grown vertically on 1/2 MS for 10 days at 22ºC, photographed, and primary root lengths and lateral root densities (number emerged lateral roots per mm of primary root) calculated using imageJ software. All phenotypic assays were performed at least three times.

Construction of transgenic plants

The *pVRN2::VRN2-GUS* and *pVRN2::Ala2-VRN2-GUS* constructs, used here to generate transgenics in the *vrn2- fca-1* background, were described previously (Gibbs *et al.*, 2018). To generate the *pER8::VIN3* construct, *VIN3* was PCR amplified from 2-week vernalized Arabidopsis seedling cDNA using attB-flanked primers, recombined into pDONOR201 using gateway BP clonase (Invitrogen; 11789020), then transferred into the destination binary vector pER8GW (Coego *et al.*, 2014) using LR clonase (Invitrogen; 11791100). Constructs were transformed into *Agrobacterium tumefaciens* (strain GV3101 pMP90), then transformed into relevant Arabidopsis lines using established floral dip method. At least 10 independent transgenic plants were selected for each construct; data from 2 independent T_3 homozygous lines are shown.

In vivo and *in vitro* protein stability analyses

Total protein was extracted from 7-day-old non-vernalized or vernalized seedlings as described previously (Gibbs *et al.*, 2011). To test the effect of hypoxia on *in vivo* protein stability, 7-day old seedlings were exposed to 1% hypoxia for 6h or 24h in a Heracell VIOS 160i incubator (Thermo Scientific), and *ADH1* expression was used as a marker gene for hypoxia efficacy. For the β-estradiol induction assays, 7 day old seedlings were transferred to liquid 1/2 MS in 6-well microtiter plates supplemented with 50μM β-estradiol (or equivalent volume DMSO control), and incubated at 22°C in the light with gentle shaking for 24 hours, before harvesting in liquid nitrogen.

The VRN2-HA *in vitro* expression construct was described previously (Gibbs *et al.*, 2018). To generate the VIN3-HA fusion driven by the T7 promoter, *VIN3* cDNA was PCR amplified from 2 week vernalized Arabidopsis seedling cDNA and directionally cloned into a modified version of the pTNT (Invitrogen) expression vector (pTNT3xHA; (Gibbs *et al.*, 2011)). Cycloheximide-chase assays were then performed using the TNT T7 Coupled Reticulocyte Lysate system (Promega; L4610) using 250ng of each construct per 25μL reaction as described previously (Gibbs *et al.*, 2018).

Immunoblotting

Equal total protein amounts were resolved by SDS–PAGE before transferring to PVDF membrane via a MiniTrans-Blot electrophoretic transfer cell (Bio-Rad). Primary antibodies were then used to probe membranes at the following dilutions: anti-HA (Sigma-Aldrich; H3663), 1:2,000; anti-GUS (Sigma-Aldrich; G5420), 1:1000. anti-FLAG (Sigma-Aldrich; F1804), 1:1000; anti-FIE (Agrisera; AS12 2616), 1:1000. HRP-conjugated anti-mouse or rabbit secondary antibodies (Santa Cruz; sc-358914 and sc-2004) were used at a titre of 1:10,000, before developing to film using ECL western blotting substrate (Pierce).

Reverse transcriptase PCR and qPCR

For semi-quantitative RT–PCR, RNA was extracted from seedlings using the RNEasy plant mini kit (Qiagen; 74904). cDNA was then synthesised with Superscript II Reverse transcriptase (Invitrogen; 18064-014) using OligodT primers. PCRs were

performed using gene- or transgene-specific primer pairs, and *ACTIN-2* was amplified for use as a loading control. For quantitative assessment of gene expression, RNA was extracted from seedlings (treated as described) and converted to cDNA as above. Real-time quantitative RT-PCR was performed in triplicate using Brilliant III UF MM SYBR QPCR Low ROX master mix (Agilent; 600892) on an AriaMx Real-Time PCR system (Agilent) according to manufacturer's instructions. Relative transcript abundance was determined by normalization to *ACTIN* and relative fold changes calculated. Data shown are mean of three biological repeats. Error bars indicate standard deviation. For primer sequences see Table S1.

Meristem measurements

6 day old Arabidopsis seedlings were stained with propidium iodide (10ug/ml) for 15 min, before rising in water. Root meristems were visualised using a Nikon A1R Eclipse Ti inverted confocal microscope. To determine meristem size, distance from the quiescent centre to the first elongated cortex cell was measured using imageJ.

Histochemical staining

To stain for β-Glucuronidase (GUS) enzyme activity, 7 day old transgenic Arabidopsis seedlings were incubated in GUS buffer [phosphate buffer(100mM) pH 7.0; Potassium Ferrycyanide (2mM); Potassium Ferrocyanide (2mM); Triton X-100 (0.1% v/v); 1mM X-Gluc solution (5-bromo-4-chloro-3-indolyl-beta-D-glucuronic acid, cyclohexylammonium salt, X-GLUC Direct)]. Samples were then incubated for 4 hours at 37ºC, cleared and fixed in 3:1 ethanol:acetic acid, then mounted on microscope slides in Hoyers solution (30g gum Arabic, 200g chloral hydrate, 20g glycerol, 50 ml water) before imaging on a light microscope.

Results

VRN2 accumulates at the shoot apex and modulates flowering dependent on photoperiod

We investigated VRN2 protein accumulation in the aerial tissues of WT Col-0 plants using a *pVRN2::VRN2-GUS* reporter line, which consists of full length VRN2 fused to β-glucuronidase, driven by ~2kb of endogenous promoter (Gibbs *et al.*, 2018). Despite

ubiquitous expression of *VRN2* mRNA across tissues (de Lucas *et al.*, 2016; Gibbs *et al.*, 2018), VRN2-GUS protein was only detected in the SAM, leaf primordia, young expanding leaves, and parts of the vasculature (Fig. 1a), which correlates with a previous study that showed enrichment of VRN2-FLAG at the shoot tip (Wood *et al.,* 2006). This localisation is remarkably similar to that observed for a *pHRPEx5:GFP-GUS* hypoxia reporter construct expressed in Col-0 seedlings of a similar age (Weits *et al.*, 2019). In contrast, *pVRN2::VRN2-GUS* in the *prt6-1* mutant accumulated throughout all tissues of the seedling, resembling *pHRPEx5:GFP-GUS* expression in lines grown under 5% O_2 (Weits *et al.*, 2019). Quantitative PCR analysis confirmed that *VRN2* expression was not significantly increased in *prt6-1* relative to WT (Fig. 1b). We therefore conclude that the N-degron pathway restricts VRN2 to the hypoxic shoot apex in the aerial tissues of Arabidopsis seedlings.

To investigate how control of VRN2 stability by the N-degron pathway regulates its functions in the shoot we took advantage of a range of genetic mutants in the Col-0 background: *vrn2-5* (which lacks full length VRN2), *prt6-1* (which ectopically accumulates VRN2, as well as other N-degron targets including ERFVIIs and presumably ZPR2), and *prt6-1 vrn2-5* (which accumulates all PRT6 N-degron substrates except for VRN2). We designed *VRN2*-specific primers upstream and downstream of the *vrn2-5* insertion site, and confirmed that the T-DNA completely abolished expression of full length *VRN2* mRNA, although a C-terminally truncated mRNA could still detected at reduced levels compared to WT (Fig. 1b and 2d). When these lines were grown under long day conditions (16h light, 8 hours dark, 22ºC), no obvious effects on phyllotaxis or morphology were observed, except for some small variations in rosette size (Fig. 1c). However, both *vrn2-5* and *prt6-1 vrn2-5* flowered earlier than Col-0 and *prt6-1* when leaf number at bolting and days to flowering were assessed (Fig. 1d,e). This indicates a repressive function for VRN2 in flowering, similar to reported roles for VRN2-like proteins in Medicago (Jaudal *et al.*, 2016). Whilst loss of VRN2 reduced time to flowering, *prt6-1* did not exhibit delayed flowering relative to WT, suggesting that ectopic accumulation of VRN2 is insufficient to enhance its effects on this process.

Col-0 is a facultative LD plant, with short photoperiods having a strong repressive effect on reproductive transition. Therefore, we also assessed flowering phenotypes under short day conditions (8h light, 16 hours dark, 22ºC). Here, all three mutants had

reduced developmental synchronicity relative to WT when leaf number at bolting was scored (i.e. broader variation in leaf numbers) (Fig. 1f). When chronological timing of flowering was determined, both *vrn2-5* and *prt6-1* flowered significantly later than Col-0, with the double mutant displaying an even stronger delay (Fig. 1g). This indicates additive positive roles in flowering for VRN2 and PRT6 under short day conditions, although a more general pleiotropic effect on quiescence cannot be ruled out. For *vrn2-5* this is opposite to what was observed under LD conditions, revealing distinct photoperiod-dependent roles for VRN2 in the shoot (Fig. 1d,e). The ERFVIIs have previously been shown to positively regulate flowering (Vicente *et al.*, 2017), which likely explains the *prt6-1* phenotype observed here. Our data reveal that VRN2 has multiple roles in regulating flowering that are separate from its role in vernalization, dependent on photoperiod, and not enhanced when its levels are ectopically increased through genetic manipulation.

VRN2 function in vernalization-dependent lines

VRN2 was initially identified as a positive regulator of the vernalization response in late-flowering Arabidopsis mutants (Chandler *et al.*, 1996). Col-0 is an early flowering ecotype that does not require vernalization due to an inactive allele of *FRIGIDA* (Johanson *et al.*, 2000), a positive regulator of *FLC* expression. To investigate how posttranslational control of VRN2 stability contributes to its functions in the vernalization response we crossed the double *prt6-1 vrn2-5* mutant to the late flowering Col-0 FRI-Sf2 introgression line (hereafter FRI-Sf2), which is almost identical to Col-0 except that it contains a dominant *FRIGIDA* allele derived from the Sf2 ecotype (Johanson *et al.*, 2000). Single and double mutants in the FRI-Sf2 background were then identified in the F_2 generation (Supporting Information Fig. S1). We confirmed increased levels of *FLC* expression in FRI-Sf2 relative to Col-0 using qPCR, and observed a concomitant delay in flowering under LD conditions (approx. 40 leaves vs 14 in Col-0) (Fig. 2a,b). Both *vrn2-5* FRI-SF2 and *prt6-1* FRI-Sf2 had slightly higher levels of *FLC* expression relative to WT FRI-Sf2, with the double mutant having the greatest increase (Fig. 2a). This corroborates previous work showing elevated *FLC* expression in late-flowering mutants carrying the *vrn2-1* mutation (Sheldon *et al.*, 2000), and indicated that single *vrn2-5* and double *prt6-1 vrn2-5*

mutants in the FRI-Sf2 background would flower later than WT, which we observed when we grew them under LD conditions (Fig. 2b). Remarkably, the *prt6-1 vrn2-5* FRI-Sf2 line flowered extremely late relative to FRI-Sf2 (>100 leaves vs ~ 40), suggesting a similar additive role for VRN2 and PRT6 in promoting flowering to that observed in the Col-0 ecotype under SD conditions (Fig. 1d,e). Increased *FLC* expression and delayed flowering in *prt6-1* FRI-Sf2 indicate that ectopic accumulation of VRN2 in the absence of cold exposure is insufficient to repress *FLC* and abolish a requirement for vernalization. Further supporting this, activity of *pFLC::FLC-GUS* was not reduced in *prt6-1* relative to a vernalization-dependent C24 parental line (Fig. 2c).

We exposed all FRI-SF2 lines to 4 weeks vernalization (4V) treatment at the seedling stage (8h light, 16 hours dark, 5ºC), before returning to LD conditions at 22ºC and assessing leaf number at bolting. Remarkably, all four lines flowered significantly earlier in response to this treatment (Fig. 2b). This was particularly striking for the *prt6-1 vrn2-5* FRI-Sf2 mutant (from >100 leaves to <30). Thus, the repressive effects induced by loss of VRN2 and PRT6 activity can be overridden by exposure to low temperatures. This was unexpected for *vrn2-5*, since VRN2 is required for vernalization, and the previously isolated *vrn2-1* mutant allele is insensitive to cold exposure (Sheldon *et al.*, 2000; Gendall *et al.*, 2001). The *vrn2-1* mutant was isolated from an EMS screen for plants that do not respond to vernalization (Chandler *et al.*, 1996), and contains a codon substitution that leads to premature truncation of VRN2 at amino acid 322 (Gendall *et al.*, 2001). In contrast, *vrn2-5* has a T-DNA insertion that is predicted to disrupt the gene downstream of the *vrn2-1* mutation site, at a residue encoding amino acid 331, and qPCR analysis confirmed that a truncated *VRN2* mRNA is expressed (Fig. 1b). Both mutations occur in the VEFS-box domain of VRN2, a critical region of the protein that is conserved in Su(z)12 homologs and required for facilitating binding and catalytic function of PRC2 (Fig. 2d) (Cao & Zhang, 2004; Ketel *et al.*, 2005). Given that *vrn2-5* has clear developmental defects related to flowering and root growth (see later), our data suggest that the *vrn2-5* allele disrupts some VRN2 functions, but in contrast to *vrn2-1* does not abolish vernalization capacity.

Ectopic stabilisation of VRN2 does not abolish the requirement for vernalization

We next investigated how regulation of VRN2 stability influences vernalization using the *vrn2-1* allele, which is in the late flowering *fca-1* mutant in Landsberg *erecta* (L*er*) (Chandler *et al.*, 1996). FCA is a component of the autonomous flowering pathway that regulates RNA-mediated chromatin silencing (Baurle *et al.*, 2007); the *fca-1* mutant has high levels of *FLC* expression, leading to a late flowering phenotype that can be overcome by vernalization. Whilst *vrn2-1 fca-1* is in the L*er* ecotype, *prt6-1* is in Col-0. Due to a lack of *prt6* mutants in L*er*, and to avoid mixing ecotypes, we instead ectopically stabilised VRN2 by introducing WT (Cys2) or mutant (Cys2Ala) variants of *pVRN2::VRN2-GUS* into *vrn2-1 fca-1*. Western blotting and histochemical staining confirmed that the Cys2Ala mutation in VRN2 is sufficient to enhance its abundance and expand its domain of accumulation throughout the seedling, similar to *prt6-1,* whilst WT VRN2 showed characteristic localization to the hypoxic shoot apex (Fig. 3a,b; two independent lines for each transgene).

We investigated flowering phenotypes in these transgenic lines relative to the untransformed *vrn2-1 fca-1* parent line. WT *pVRN2::VRN2-GUS* and mutant *pVRN2::Ala2-VRN2-GUS* plants all flowered late under LD conditions, similar to the *vrn2-1 fca-1*, with all lines showing low synchronicity in leaf number at bolting (Fig. 3c). We exposed these lines to increasing lengths of time at 5 ºC (2, 3 and 4 weeks). As expected, the *vrn2-1 fca-1* mutant was insensitive to vernalization treatment. However, all four transgenics flowered earlier in a dose dependent manner, signifying that the WT and mutant *pVRN2::VRN2-GUS* constructs can functionally compensate for the *vrn2-1* mutation. Extended exposure to cold also led to greater synchronicity of flowering for all lines tested. The mutant *pVRN2::Ala2-VRN2-GUS* plants had a slightly enhanced response to shorter cold exposure times, which was most pronounced following three weeks of vernalization. However, by four weeks all transgenic lines flowered at a similar time. We conclude therefore that ectopic stabilisation of VRN2 by mutating its N-degron is insufficient to significantly enhance its function during vernalization relative to WT.

VRN2 stability in relation to other PRC2 components and the VIN3 co-factor

Our data reveal that VRN2 accumulation in *prt6-1* or through N-terminal mutagenesis does not lead to increased VRN2 function with regards to photoperiod- or

vernalization-associated flowering. The former could be explained by the fact that VRN2 is already stabilised in regions of the plant – i.e. hypoxic niches – where this function is established, with enhanced abundance outside these domains having no further influence. The latter is likely due to a lack of other cold-specific factors that are required for efficient silencing of *FLC* (Costa & Dean, 2019). Nonetheless, these findings prompted us to investigate the relationship between VRN2 stability and the abundance of other core PRC2 components and accessory proteins during cold exposure, hypoxia, and in the *prt6-1* mutant.

The Arabidopsis PRC2 complex consists of four core subunits; three of these are encoded by multiple family members, but one of these – FIE – is not (Fig. 4a). We therefore used FIE protein as a proxy for relative PRC2 abundance in relation to VRN2 accumulation. Western blot analysis showed that whilst VRN2 accumulated to high levels in *prt6-1* relative to WT, the amount of total FIE protein was unaltered (Fig. 4b). During cold exposure, however, FIE abundance increased in a dose-dependent manner, and depleted again upon return to warm temperatures, similar to VRN2 (Fig. 4c). It was previously also shown that CLF and SWN methyltransferases accumulate during cold exposure (Wood *et al.*, 2006). We also saw similar increases in both VRN2-GUS and FIE abundance in response to hypoxia (Fig. 4d). This suggests that genetic enhancement of VRN2 levels (i.e. in *prt6-1*) might be insufficient to stimulate enhanced VRN2-PRC2 activity due to a lack of a concomitant increase of other complex subunits or interaction partners, which only occurs when VRN2 accumulates in environmental contexts (i.e. cold exposure or hypoxia).

We also examined the dynamics of the VRN2-PRC2 cofactor VIN3. VIN3 is a key player in the vernalization response (Sung & Amasino, 2004), which is transcriptionally induced by cold temperatures and binds specifically to VRN2-PRC2 along with VRN5 to potentiate methylation of the *FLC* nucleation site (Greb *et al.*, 2007; Costa & Dean, 2019). Interestingly, *VIN3* was also previously shown to be upregulated by hypoxia, where it contributes to hypoxia resilience, similar to VRN2 (Bond *et al.*, 2009; Gibbs *et al.*, 2018). We confirmed cold-responsive induction of *VIN3* expression (Fig. 4e). However, we found that 6h exposure to 1% O_2 was not sufficient to induce *VIN3*, despite enhancing VRN2-GUS stability and increasing *ADH1* expression >100 fold, indicating different timescales for regulation in response to O_2 deprivation (Fig. 4d,f). To test if longer hypoxic treatments trigger *VIN3* induction we exposed both WT and

prt6-1 seedlings to 1% O_2 for 24 h. However, we saw a reduction rather than an increase in *VIN3* expression, despite *ADH1* mRNA levels confirming the efficacy of the hypoxia treatment (Fig. 4g). Furthermore, *VIN3* mRNA levels were not elevated in *prt6-1* relative to WT (Fig. 4e,g), and *VIN3* does not appear in published hypoxia microarray datasets (Gibbs *et al.,* 2011), indicating that transcriptional control of *VIN3* is not linked to the canonical mechanism for hypoxia-responsive gene induction through ERFVIIs. As such, a mechanistic connection between VRN2 and *VIN3* under hypoxia is still unclear.

It had previously been proposed that cold-triggered induction of *VIN3* (Fig. 4e) might enhance the abundance of PRC2 subunits during vernalization through binding and stabilising the complex (Wood *et al.*, 2006). We tested the possibility that VIN3 promotes VRN2 stability - e.g. through steric shielding of the VRN2 N-degron - by co-expressing VIN3-HA and VRN2-HA in a cell free rabbit reticulocyte system that contains a functional Arg N-degron pathway (Gibbs *et al.*, 2011), and monitoring protein levels over time following treatment with the translational inhibitor cycloheximide (CHX) (Fig. 4h). Here, VRN2-HA was unstable even in the presence of VIN3-HA. In contrast, when VRN2-HA was co-incubated with the proteasome inhibitor bortezomib without VIN3-HA, its turnover was inhibited. Thus, VIN3 alone is not sufficient to stabilise VRN2. We also introduced β-estradiol-inducible *VIN3* constructs into the previously described *pVRN2::VRN2-FLAG* Arabidopsis line, to test if ectopic induction of *VIN3* in planta affects VRN2 abundance. However, despite clear induction of *VIN3* expression in the presence of β-estradiol, no obvious increase in VRN2-FLAG stability was observed (Fig. 4i). Together, these data suggest that whilst VIN3 is required for vernalization through its association with VRN2-PRC2, it does not promote increased stability of VRN2.

The PRT6 N-degron pathway confines VRN2 to discrete root tissues and negatively regulates root growth

In addition to assessing the spatiotemporal pattern of VRN2 localisation in aerial tissues, we investigated VRN2 abundance in the root system of seedlings. WT VRN2-GUS was detected in the primary root (PR) meristem zone, in LRPs and emerged LRs, and parts of the vasculature (Fig. 5a). In contrast, mutant Ala2-VRN2-GUS, and WT

VRN2-GUS in *prt6-1*, had expanded domains of accumulation, localising throughout the root (Fig. 5a). Quantitative RT-PCR analysis confirmed that *VRN2* expression levels are not enhanced in WT root tips relative to the main root, nor in *prt6-1* root tips compared to WT (Fig. 5b). Thus, similar to in aerial tissues, the N-degron pathway post-translationally restricts VRN2 protein to discrete regions of roots.

Mid-to-late stage LRPs have recently been shown to be hypoxic (Shukla *et al.*, 2019). Interestingly, in contrast to the SAM, the root meristem of young, establishing seedlings may not be hypoxic, since anaerobic gene expression is not enriched in this region and the ERFVII RAP2.12 does not accumulate there (Hartman *et al.*, 2019; Weits *et al.*, 2019). However, in the PR tip of older seedlings, ERFVIIs are stable (Holdsworth *et al.*, 2019). Thus, since VRN2 mRNAs are not enriched in this region relative to other parts of the root (Fig. 5b), the accumulation of VRN2 protein may be due to other factors blocking VRN2 proteolysis, differential sensitivities to O_2 availability in this tissue, or age-dependent variability in N-degron pathway activity (Giuntoli *et al.*, 2017).

Given the localisation of VRN2 to LRPs and the PR meristem, we investigated root architecture in *vrn2-5*, *prt6-1* and *prt6-1 vrn2-5* relative to Col-0. When grown on vertical agar plates, seedlings of the *vrn2-5* mutant had significantly longer PRs than WT, whilst *prt6-1* mutant roots were shorter (Fig. 5c,d). The *prt6-1 vrn2*-5 mutant had PRs of a similar length to WT, indicating that stable VRN2 contributes to the reduced root length phenotype of *prt6-1*. We also observed enhanced meristem size in *vrn2-5* relative to WT, which correlates with the increased PR lengths observed in this line (Fig. 5f,g). A similar pattern across the mutants was observed when emerged lateral root (LR) densities were scored: *vrn2-5* had increased LR density, *prt6-1* reduced density, and the double mutant had an intermediate phenotype (Fig. 5e). *prt6-1* was recently shown to have reduced LR density due to an accumulation of ERFVIIs, that repress LR production (Shukla *et al.*, 2019). Our data suggest that repression of LRs in *prt6-1* is controlled by stable VRN2 as well as ERFVIIs.

To further investigate the role for VRN2 in regulating root system architecture, we also examined root growth in the *vrn2-1 fca-1* mutant, as well as *vrn2-1 fca-1* complemented with WT *pVRN2::VRN2-GUS* or mutant stable *pVRN2::Ala2-VRN2-GUS* (Fig. 3a,b). Here, both transgenes led to a reduction in PR length and emerged

LR density relative to *vrn2-1 fca-1*, but this was most pronounced in the *pVRN2::Ala2-VRN2-GUS* line (Fig. 6a,b,c). This therefore corroborates our findings in Col-0, identifying VRN2 as a negative regulator of root growth, and indicates that – in contrast to flowering - ectopic stabilisation of VRN2 is sufficient to enhance its function in roots.

Discussion

Here we investigated how control of VRN2 by the PCO dependent branch of the PRT6 N-degron pathway relates to its localisation and functions in plant development. Our data indicate that posttranslational control of VRN2 plays a key role in restricting its accumulation to specific regions of the shoot and root that are hypoxic, where it contributes to the regulation of flowering time and repression of root growth. These roles are separate from its function in vernalization, which is potentiated in response to cold temperatures that inhibit proteolysis to enhance VRN2 abundance throughout the plant. Thus, our findings suggest that the N-degron of VRN2 has distinct roles in limiting VRN2 abundance to discrete tissues, whilst also permitting accumulation in response to environmental inputs where it carries out a different set of context-specific functions.

In the early flowering Col-0 ecotype, VRN2 has opposing roles in modulating flowering, dependent on photoperiod: Under long days VRN2 is repressive, whilst under short days it has a positive function (Fig. 1). In late flowering FRI-Sf2, the positive function of VRN2 also manifests under long days (Fig. 2). We found that ectopic stabilisation of VRN2 did not enhance the photoperiod-dependent functions of VRN2 (Fig. 3). This is likely because such functions are linked to VRN2 activity in the shoot apex, where it is already stable due to maintenance of a hypoxic niche in this region. How VRN2 differentially influences flowering remains to be determined. Photo-dependent flowering is regulated by a complex network of floral regulators, which includes components of the circadian clock and light receptors, which converge on the zinc finger transcription factor *CONSTANS* that in turn modulates levels of the Florigen gene *FLOWERING LOCUS T* (Song *et al.*, 2015). VRN2 may contribute to the epigenetic regulation of any or several components in this pathway, or alternatively it could have pleiotropic effects on this developmental process related to growth and

quiescence. Future analysis of genome-wide methylation targets of VRN2-PRC2 may shed light on this.

VRN2 also had a restricted pattern of accumulation in root tissues, where the PCO branch of the PRT6 N-degron pathway limits its abundance to the root meristem zone and LRPs to repress root development (Fig. 5,6). Plants with mutations in VRN2 (*vrn2-5* and *vrn2-1*) had increased PR lengths and emerged LR densities, whilst the *prt6-1* mutant and plants expressing stable Ala2-VRN2-GUS had opposite root phenotypes – i.e. shorter PRs and a reduced LR density. This effect was partially reverted in the *prt6-1 vrn2-5* double mutant, indicating that ectopic accumulation of VRN2 in roots does lead to enhanced function, in contrast to the situation in aerial tissues. It was previously reported that different PRC2 subunits have distinct and opposing roles in the control of root development: mutations in SWN and MSI1 cause smaller PRs with reduced meristem size, whilst a CLF mutant (*clf29*) had longer roots and significantly increased number of cells in the meristem (de Lucas *et al.*, 2016). We observed enhanced meristem size in *vrn2-5* relative to WT, which is similar to the previous observation in *clf29*. Thus, it is possible that the repressive role of VRN2 in root system architecture is linked to the CLF methyltransferase.

Hypoxic niches have recently been identified in pre-emerged LRPs, which likely explains why VRN2 accumulates in these regions (Shukla *et al.*, 2019). However, in contrast to the shoot meristem, root meristems are yet to be defined as hypoxic when assayed in normoxia (Weits *et al.*, 2019), and so it is possible that VRN2 accumulation in the root tip is linked to alternative mechanisms inhibiting its proteolysis (e.g. perhaps steric shielding of the N-degron by a tissue-specific binding partner). Alternatively, root meristems may show different sensitivity to O_2, as root tip growth occurs in the soil, which is likely to be an hypoxic environment (Abbas *et al.*, 2015). Hypoxic niches in LRPs were recently shown to enhance ERFVIIs, which inhibit LR development through repressing the expression of the auxin-associated genes *LBD16/18*, *IAA29* and *PUCHI* (Shukla *et al.*, 2019). It will be important to determine if any of these same genes are also repressed at the epigenetic level through the action of locally stabilised VRN2, or whether separate targets are involved.

VRN2 is well characterised as a positive regulator of the vernalization response, accumulating during cold exposure to facilitate methylation and silencing of *FLC*.

However, ectopic accumulation of VRN2 (in either *prt6-1* or through N-terminal mutagenesis) did not repress *FLC* or abolish the requirement for vernalization (Fig. 2 and 3). This was perhaps not unexpected, since other cold-specific protein and regulatory lncRNAs are required for the epigenetic repression of *FLC* (Costa & Dean, 2019). However, this led us to investigate in further detail the relationship between VRN2 abundance and the presence of other PRC2 subunits that are necessary for VRN2 to carry out PRC2-associated functions. When VRN2 is ectopically enhanced, levels of the core PRC2 component FIE do not change (Fig. 4), which indicates an over accumulation of 'free' VRN2 protein. In contrast, cold- and hypoxia-triggered increases in VRN2 abundance were accompanied by higher levels of FIE. Thus, when VRN2 is stabilised outside of meristems in response to environmental signals, there is the capacity for a similar overall increase in VRN2-PRC2 that cannot take place when VRN2 accumulates out of context. The PHD protein VIN3 was previously shown to be transcriptionally induced by both cold and hypoxia, two environmental conditions that also inhibit VRN2 proteolysis. Whilst we also observed cold induction of *VIN3* transcripts, we did not see an increase in *VIN3* expression in response to hypoxia treatment (Sung & Amasino, 2004; Bond *et al.*, 2009; Gibbs *et al.*, 2018). However, it should be noted that here we used 1% O_2, whereas Bond *et al.* (2009) used 0.1%, suggesting that perhaps *VIN3* induction requires extremely low O_2 availability, or even anoxia. *VIN3* expression was not increased in *prt6-1* relative to Col-0, further highlighting that VRN2-PRC2 binding partners required for vernalization are not available when VRN2 artificially accumulates. It was previously postulated that VIN3 might promote VRN2-PRC2 increases during long term cold exposure, through binding and enhancing stability of the complex. We explored this possibility by investigating the effect of VIN3 on VRN2 stability *in vitro* and *in planta*. VIN3 did not stabilise VRN2, which suggests alternative mechanisms promoting observed increases in PRC2 components in response to cold temperatures (Fig. 4 and (Wood *et al.*, 2006). Collectively, our data indicate that functions for VRN2 outside of meristems are only activated when it accumulates in appropriate environmental contexts due to a requirement for other specific binding factors.

The *vrn2-5* mutant used in this study displayed several phenotypes related to both flowering and root development. This mutant was also previously shown to influence hypoxia tolerance and maternal effects on seed dormancy (Auge *et al.*, 2017; Gibbs

et al., 2018). However, in contrast to the *vrn2-1*, *vrn2-5* was still able to fully respond to vernalization treatment, indicating that *vrn2-5* disrupts some but not all VRN2 functions. The VEFS domain in Su(z)12 is required for binding to PRC2 and stimulating methyltransferase activity (Cao & Zhang, 2004). Full deletion of the VEFS domain abolishes the capacity for Su(z)12 to associate with catalytic Ez subunit in Drosophila. In contrast, a series of point mutations at different positions in the VEFS box of Su(z)12 affected PRC2 activity to different degrees (Ketel *et al.*, 2005). A D593A mutation in the latter half of the VEFS-box had no effect on PRC2 assembly or enzymatic function, whilst a D550A mutation earlier in the sequence had a modest effect on methyltransferase activity (Ketel *et al.*, 2005). In contrast, an E546A mutation just 4 residues upstream of D550 almost completely abolished PRC2 function. Thus it is plausible that the different positions of mutation in *vrn2-1* and *vrn2-5* could differentially affect VRN2 activity, perhaps through modulating binding stoichiometries, as has been observed for other Su(12z) mutations previously (Birve *et al.*, 2001). It will now be important to develop further knockouts of VRN2 in different ecotypes, for example through the use of CRISPR, to help dissect its different functions in development and environmental response.

In conclusion, we show that VRN2 has multiple functions in plant development that are linked to the control of its abundance through the PCO branch of the PRT6 N-degron pathway. Co-option of Su(z)12 to this proteolytic system allows plants to control spatial abundance and function of VRN2 by limiting it to endogenous hypoxic niches, whilst also coupling its accumulation to the perception of specific environmental cues where it adopts a separate set of functions. In this way, regulation of VRN2 by the PRT6 N-degron pathway is similar to that for ERFVIIs, which also have dual functionality in tissue-specific coordination of development, and broader environment-triggered regulation of stress responses.

Acknowledgements

This work was supported by a European Research Council Starter Grant [ERC-STG 715441-GasPlaNt] to D.J.G, grants from the Biotechnology and Biological Sciences Research Council to D.J.G [BB/M020568/1] and M.J.H [BB/M007820/1 and BB/M029441/1], and an EMBO Long Term Fellowship [ALTF 219-2018] to A.M.L.

Author contributions

D.J.G, A.M.L. and M.J.H. designed and conceived the research. D.J.G., A.M.L., H.M.T., M.B., C.S., R.E., G.K., O.A., and M.J.H conducted experiments. D.J.G, A.M.L., and M.J.H. analysed data. D.J.G. wrote the manuscript with input from all authors.

References

Abbas M, Berckhan S, Rooney DJ, Gibbs DJ, Conde JV, Correia CS, Bassel GW, Marin-de la Rosa N, Leon J, Alabadi D, et al. 2015. Oxygen Sensing Coordinates Photomorphogenesis to Facilitate Seedling Survival. *Current Biology* **25**(11): 1483-1488.

Auge GA, Blair LK, Neville H, Donohue K. 2017. Maternal vernalization and vernalization-pathway genes influence progeny seed germination. *New Phytol* **216**(2): 388-400.

Bailey-Serres J, Fukao T, Gibbs DJ, Holdsworth MJ, Lee SC, Licausi F, Perata P, Voesenek LA, van Dongen JT. 2012. Making sense of low oxygen sensing. *Trends Plant Sci* **17**(3): 129-138.

Baurle I, Smith L, Baulcombe DC, Dean C. 2007. Widespread role for the flowering-time regulators FCA and FPA in RNA-mediated chromatin silencing. *Science* **318**(5847): 109-112.

Birve A, Sengupta AK, Beuchle D, Larsson J, Kennison JA, Rasmuson-Lestander A, Muller J. 2001. Su(z)12, a novel Drosophila Polycomb group gene that is conserved in vertebrates and plants. *Development* **128**(17): 3371-3379.

Bond DM, Wilson IW, Dennis ES, Pogson BJ, Jean Finnegan E. 2009. VERNALIZATION INSENSITIVE 3 (VIN3) is required for the response of Arabidopsis thaliana seedlings exposed to low oxygen conditions. *Plant J* **59**(4): 576-587.

Borisjuk L, Rolletschek H. 2009. The oxygen status of the developing seed. *New Phytol* **182**(1): 17-30.

Cao R, Zhang Y. 2004. SUZ12 is required for both the histone methyltransferase activity and the silencing function of the EED-EZH2 complex. *Mol Cell* **15**(1): 57-67.

Chandler J, Wilson A, Dean C. 1996. Arabidopsis mutants showing an altered response to vernalization. *Plant J* **10**(4): 637-644.

Chen LJ, Diao ZY, Specht C, Sung ZR. 2009. Molecular evolution of VEF-domain-containing PcG genes in plants. *Mol Plant* **2**(4): 738-754.

Coego A, Brizuela E, Castillejo P, Ruiz S, Koncz C, del Pozo JC, Pineiro M, Jarillo JA, Paz-Ares J, Leon J, et al. 2014. The TRANSPLANTA collection of Arabidopsis lines: a resource for functional analysis of transcription factors based on their conditional overexpression. *Plant J* **77**(6): 944-953.

Considine MJ, Diaz-Vivancos P, Kerchev P, Signorelli S, Agudelo-Romero P, Gibbs DJ, Foyer CH. 2017. Learning To Breathe: Developmental Phase Transitions in Oxygen Status. *Trends Plant Sci* **22**(2): 140-153.

Costa S, Dean C. 2019. Storing memories: the distinct phases of Polycomb-mediated silencing of Arabidopsis FLC. *Biochem Soc Trans*.

de Lucas M, Pu L, Turco G, Gaudinier A, Morao AK, Harashima H, Kim D, Ron M, Sugimoto K, Roudier F, et al. 2016. Transcriptional Regulation of Arabidopsis Polycomb Repressive Complex 2 Coordinates Cell-Type Proliferation and Differentiation. *Plant Cell* **28**(10): 2616-2631.

de Marchi R, Sorel M, Mooney B, Fudal I, Goslin K, Kwasniewska K, Ryan PT, Pfalz M, Kroymann J, Pollmann S, et al. 2016. The N-end rule pathway regulates pathogen responses in plants. *Sci Rep* **6**: 26020.

Dissmeyer N. 2019. Conditional Protein Function via N-Degron Pathway-Mediated Proteostasis in Stress Physiology. *Annu Rev Plant Biol* **70**: 83-117.

Gendall AR, Levy YY, Wilson A, Dean C. 2001. The VERNALIZATION 2 gene mediates the epigenetic regulation of vernalization in Arabidopsis. *Cell* **107**(4): 525-535.

Gibbs D, Vicente Conde J, Berckhan S, Mendiondo GM, Prasad G, Holdsworth MJ. 2015. Group VII Ethylene Response Factors co-ordinate oxygen and nitric oxide signal transduction and stress responses in plants. *Plant Physiol*.

Gibbs DJ, Bacardit J, Bachmair A, Holdsworth MJ. 2014a. The eukaryotic N-end rule pathway: conserved mechanisms and diverse functions. *Trends Cell Biol*.

Gibbs DJ, Bailey M, Tedds HM, Holdsworth MJ. 2016. From start to finish: amino-terminal protein modifications as degradation signals in plants. *New Phytol* **211**(4): 1188-1194.

Gibbs DJ, Lee SC, Isa NM, Gramuglia S, Fukao T, Bassel GW, Correia CS, Corbineau F, Theodoulou FL, Bailey-Serres J, et al. 2011. Homeostatic response to hypoxia is regulated by the N-end rule pathway in plants. *Nature* **479**(7373): 415-418.

Gibbs DJ, Md Isa N, Movahedi M, Lozano-Juste J, Mendiondo GM, Berckhan S, Marin-de la Rosa N, Vicente Conde J, Sousa Correia C, Pearce SP, et al. 2014b. Nitric Oxide Sensing in Plants Is Mediated by Proteolytic Control of Group VII ERF Transcription Factors. *Mol Cell*.

Gibbs DJ, Tedds HM, Labandera A-M, Bailey M, White MD, Hartman S, Sprigg C, Mogg SL, Osborne R, Dambire C, et al. 2018. Oxygen-dependent proteolysis regulates the stability of angiosperm polycomb repressive complex 2 subunit VERNALIZATION 2. *Nat Commun* **9**(1): 5438.

Giuntoli B, Shukla V, Maggiorelli F, Giorgi FM, Lombardi L, Perata P, Licausi F. 2017. Age-dependent regulation of ERF-VII transcription factor activity in Arabidopsis thaliana. *Plant Cell Environ* **40**(10): 2333-2346.

Greb T, Mylne JS, Crevillen P, Geraldo N, An H, Gendall AR, Dean C. 2007. The PHD finger protein VRN5 functions in the epigenetic silencing of Arabidopsis FLC. *Curr Biol* **17**(1): 73-78.

Hartman S, Liu Z, van Veen H, Vicente J, Reinen E, Martopawiro S, Zhang H, van Dongen N, Bosman F, Bassel GW, et al. 2019. Ethylene-mediated nitric oxide depletion pre-adapts plants to hypoxia stress. *Nat Commun* **10**(1): 4020.

Hennig L, Derkacheva M. 2009. Diversity of Polycomb group complexes in plants: same rules, different players? *Trends Genet* **25**(9): 414-423.

Holdsworth MJ, Vicente J, Sharma G, Abbas M, Zubrycka A. 2019. The plant N-degron pathways of ubiquitin-mediated proteolysis. *J Integr Plant Biol*.

Ikeuchi M, Iwase A, Rymen B, Harashima H, Shibata M, Ohnuma M, Breuer C, Morao AK, de Lucas M, De Veylder L, et al. 2015. PRC2 represses dedifferentiation of mature somatic cells in Arabidopsis. *Nat Plants* **1**: 15089.

Jaudal M, Zhang L, Che C, Hurley DG, Thomson G, Wen J, Mysore KS, Putterill J. 2016. MtVRN2 is a Polycomb VRN2-like gene which represses the transition to flowering in the model legume Medicago truncatula. *Plant J* **86**(2): 145-160.

Johanson U, West J, Lister C, Michaels S, Amasino R, Dean C. 2000. Molecular analysis of FRIGIDA, a major determinant of natural variation in Arabidopsis flowering time. *Science* **290**(5490): 344-347.

Kelliher T, Walbot V. 2012. Hypoxia triggers meiotic fate acquisition in maize. *Science* **337**(6092): 345-348.

Ketel CS, Andersen EF, Vargas ML, Suh J, Strome S, Simon JA. 2005. Subunit contributions to histone methyltransferase activities of fly and worm polycomb group complexes. *Mol Cell Biol* **25**(16): 6857-6868.

Lee I, Aukerman MJ, Gore SL, Lohman KN, Michaels SD, Weaver LM, John MC, Feldmann KA, Amasino RM. 1994. Isolation of LUMINIDEPENDENS: a gene involved in the control of flowering time in Arabidopsis. *Plant Cell* **6**(1): 75-83.

Licausi F, Kosmacz M, Weits DA, Giuntoli B, Giorgi FM, Voesenek LA, Perata P, van Dongen JT. 2011. Oxygen sensing in plants is mediated by an N-end rule pathway for protein destabilization. *Nature* **479**(7373): 419-422.

Lin CC, Chao YT, Chen WC, Ho HY, Chou MY, Li YR, Wu YL, Yang HA, Hsieh H, Lin CS, et al. 2019. Regulatory cascade involving transcriptional and N-end rule pathways in rice under submergence. *Proc Natl Acad Sci U S A* **116**(8): 3300-3309.

Margueron R, Reinberg D. 2011. The Polycomb complex PRC2 and its mark in life. *Nature* **469**(7330): 343-349.

Meitha K, Agudelo-Romero P, Signorelli S, Gibbs DJ, Considine JA, Foyer CH, Considine MJ. 2018. Developmental control of hypoxia during bud burst in grapevine. *Plant Cell Environ* **41**(5): 1154-1170.

Meitha K, Konnerup D, Colmer TD, Considine JA, Foyer CH, Considine MJ. 2015. Spatio-temporal relief from hypoxia and production of reactive oxygen species during bud burst in grapevine (Vitis vinifera). *Ann Bot* **116**(4): 703-711.

Mozgova I, Kohler C, Hennig L. 2015. Keeping the gate closed: functions of the polycomb repressive complex PRC2 in development. *Plant J* **83**(1): 121-132.

Ohad N, Yadegari R, Margossian L, Hannon M, Michaeli D, Harada JJ, Goldberg RB, Fischer RL. 1999. Mutations in FIE, a WD polycomb group gene, allow endosperm development without fertilization. *Plant Cell* **11**(3): 407-416.

Roszak P, Kohler C. 2011. Polycomb group proteins are required to couple seed coat initiation to fertilization. *Proc Natl Acad Sci U S A* **108**(51): 20826-20831.

Schmidt RR, Fulda M, Paul MV, Anders M, Plum F, Weits DA, Kosmacz M, Larson TR, Graham IA, Beemster GTS, et al. 2018. Low-oxygen response is triggered by an ATP-dependent shift in oleoyl-CoA in Arabidopsis. *Proc Natl Acad Sci U S A* **115**(51): E12101-E12110.

Sheldon CC, Hills MJ, Lister C, Dean C, Dennis ES, Peacock WJ. 2008. Resetting of FLOWERING LOCUS C expression after epigenetic repression by vernalization. *Proc Natl Acad Sci U S A* **105**(6): 2214-2219.

Sheldon CC, Rouse DT, Finnegan EJ, Peacock WJ, Dennis ES. 2000. The molecular basis of vernalization: the central role of FLOWERING LOCUS C (FLC). *Proc Natl Acad Sci U S A* **97**(7): 3753-3758.

Shukla V, Lombardi L, Iacopino S, Pencik A, Novak O, Perata P, Giuntoli B, Licausi F. 2019. Endogenous Hypoxia in Lateral Root Primordia Controls Root Architecture by Antagonizing Auxin Signaling in Arabidopsis. *Mol Plant* **12**(4): 538-551.

Simon JA, Kingston RE. 2009. Mechanisms of polycomb gene silencing: knowns and unknowns. *Nat Rev Mol Cell Biol* **10**(10): 697-708.

Song YH, Shim JS, Kinmonth-Schultz HA, Imaizumi T. 2015. Photoperiodic flowering: time measurement mechanisms in leaves. *Annu Rev Plant Biol* **66**: 441-464.

Sung S, Amasino RM. 2004. Vernalization in Arabidopsis thaliana is mediated by the PHD finger protein VIN3. *Nature* **427**(6970): 159-164.

van Dongen JT, Licausi F. 2015. Oxygen Sensing and Signaling. *Annu Rev Plant Biol*.

Vicente J, Mendiondo GM, Movahedi M, Peirats-Llobet M, Juan YT, Shen YY, Dambire C, Smart K, Rodriguez PL, Charng YY, et al. 2017. The Cys-Arg/N-End Rule Pathway Is a General Sensor of Abiotic Stress in Flowering Plants. *Curr Biol* **27**(20): 3183-3190 e3184.

Vicente J, Mendiondo GM, Pauwels J, Pastor V, Izquierdo Y, Naumann C, Movahedi M, Rooney D, Gibbs DJ, Smart K, et al. 2019. Distinct branches of the N-end rule pathway modulate the plant immune response. *New Phytol* **221**(2): 988-1000.

Weits DA, Giuntoli B, Kosmacz M, Parlanti S, Hubberten HM, Riegler H, Hoefgen R, Perata P, van Dongen JT, Licausi F. 2014. Plant cysteine oxidases control the oxygen-dependent branch of the N-end-rule pathway. *Nat Commun* **5**: 3425.

Weits DA, Kunkowska AB, Kamps NCW, Portz KMS, Packbier NK, Nemec Venza Z, Gaillochet C, Lohmann JU, Pedersen O, van Dongen JT, et al. 2019. An apical hypoxic niche sets the pace of shoot meristem activity. *Nature* **569**(7758): 714-717.

White MD, Klecker M, Hopkinson RJ, Weits DA, Mueller C, Naumann C, O'Neill R, Wickens J, Yang J, Brooks-Bartlett JC, et al. 2017. Plant cysteine oxidases are dioxygenases that directly enable arginyl transferase-catalysed arginylation of N-end rule targets. *Nat Commun* **8**: 14690.

Wood CC, Robertson M, Tanner G, Peacock WJ, Dennis ES, Helliwell CA. 2006. The Arabidopsis thaliana vernalization response requires a polycomb-like protein complex that also includes VERNALIZATION INSENSITIVE 3. *Proc Natl Acad Sci U S A* **103**(39): 14631-14636.

Yadegari R, Kinoshita T, Lotan O, Cohen G, Katz A, Choi Y, Katz A, Nakashima K, Harada JJ, Goldberg RB, et al. 2000. Mutations in the FIE and MEA genes that encode interacting polycomb proteins cause parent-of-origin effects on seed development by distinct mechanisms. *Plant Cell* **12**(12): 2367-2382.

Yang H, Berry S, Olsson TSG, Hartley M, Howard M, Dean C. 2017. Distinct phases of Polycomb silencing to hold epigenetic memory of cold in Arabidopsis. *Science* **357**(6356): 1142-1145.

Yang J, Lee S, Hang R, Kim SR, Lee YS, Cao X, Amasino R, An G. 2013. OsVIL2 functions with PRC2 to induce flowering by repressing OsLFL1 in rice. *Plant J* **73**(4): 566-578.

Yoshida N, Yanai Y, Chen L, Kato Y, Hiratsuka J, Miwa T, Sung ZR, Takahashi S. 2001. EMBRYONIC FLOWER2, a novel polycomb group protein homolog, mediates shoot development and flowering in Arabidopsis. *Plant Cell* **13**(11): 2471-2481.

Zhang H, Gannon L, Jones PD, Rundle CA, Hassall KL, Gibbs DJ, Holdsworth MJ, Theodoulou FL. 2018. Genetic interactions between ABA signalling and the Arg/N-end rule pathway during Arabidopsis seedling establishment. *Sci Rep* **8**(1): 15192.

Figure Legends

Figure 1: VRN2 accumulates in the shoot apex and modulates flowering dependent on photoperiod. (a) Histochemical staining of col-0 and *prt6-1* seedlings expressing the *pVRN2::VRN2-GUS* translational reporter: i, 7 day old seedlings, scale bar = 1mm; ii, 4-day old seedlings, bar = 200µm. Arrow head: shoot apical meristem. **(b)** Quantitative RT-PCR (qPCR) of *VRN2* in lines indicated, using primers located upstream (P1) and downstream (P2) of the *vrn2-5* T-DNA insertion. Expression levels are shown relative to WT for each primer set, and ANOVA was carried out separately on P1 and P2 data. Data are average of three biological replicates. For location of P1 and P2 in *VRN2* see Figure 2d. **(c)** Representative images of 4-week old rosettes grown under long day (LD) conditions. Bar = 1cm. **(d)** Rosette leaf number and **(e)** days to flowering under LD conditions (n=15-22 per genotype). **(f)** Rosette leaf number and **(g)** days to flowering under short day (SD) conditions (n=11-13 per genotype).

Light (L) to dark (D) ratios are indicated. Box and whiskers plots show max and min, 25th to 75th percentiles, median and mean (+). Letters indicate one way ANOVA; Tukey's test (p<0.05-0.01).

Figure 2: VRN2 function in vernalization-dependent lines. (a) Quantitative RT-PCR (qPCR) of *FLC* in in Col-0 and Col-0 FRI-Sf2 WT and mutant backgrounds. Expression levels are shown relative to Col-0 WT. Data are average of three biological replicates. **(b)** Rosette leaf number at flowering in Col-0 FRI-Sf2 WT and mutant lines under non-vernalizing (0V) or 4-week vernalizing (4V) conditions (n=8-12 per genotype). **(c)** Histochemical staining of the *pFLC::FLC-GUS* translational reporter in C24 (WT) and *prt6-1*. Scale bar = 1mm. **(d)** Schematic diagram of the *VRN2* locus and the derived protein, showing the functionally important C-terminal VEFS-box domain. The location of *vrn2-1* and *vrn2-5* mutations is indicated along with the predicted amino acid (aa) positions disrupted in VRN2. Blue arrows show position of primer pairs used for qPCR in Figure 1b. Box and whiskers plots in (a) and (b) show max and min, 25th to 75th percentiles, median and mean (+). Letters indicate one way ANOVA; Tukey's test (p<0.05-0.01).

Figure 3: Ectopic stabilisation of VRN2 does not abolish the requirement for vernalization. (a) Anti-GUS western blot and **(b)** histochemical staining of 7 day old *vrn2-1 fca-1* seedlings expressing either WT or mutant (Ala2) *pVRN2::VRN2-GUS*. CBB, coomassie brilliant blue. Scale bar = 1mm **(c)** Rosette leaf number at flowering for L*er*, *vrn2-1 fca-1*, and *vrn2- fca-1* expressing WT or mutant (Ala2) *pVRN2::VRN2-GUS* under non vernalization conditions (0 weeks) or following 2 to 4 weeks vernalization (n=8-10 per genotype per condition). Box and whiskers plots in (c) and (d) show max and min, 25th to 75th percentiles, median and mean (+). Letters indicate one way ANOVA; Tukey's test (p<0.05-0.01).

Figure 4: VRN2 stability in relation to other PRC2 subunits and the VIN3 co-factor. (a) Diagram showing Arabidopsis proteins making up the four core subunits of PRC2. **(b)** Steady state protein and mRNA levels of VRN2-GUS and FIE in Col-0 and

prt6-1 expressing *pVRN2::VRN2-GUS*. **(c)** Steady state protein levels of VRN2-GUS and FIE in vernalized (0 – 4 weeks) Col-0 seedlings expressing *pVRN2:VRN2-GUS*. 4+1 refers to 1 week recover at 22°C following 4 weeks cold exposure. **(d)** Steady state protein and mRNA levels of VRN2-GUS, FIE, and *VIN3* in 7 day old *pVRN2::VRN2-GUS* seedlings under normoxia (21% O_2) or following 6h hypoxia (1% O_2) treatment. **(e)** RT-PCR of *VIN3* in col-0 or *prt6-1* +/- 4 weeks vernalization treatment. **(f)** Quantitative RT-PCR (qPCR) of *ADH1* for samples in figure (d), confirming efficacy of hypoxia treatment. Data are average of 3 biological replicates. **(g)** qPCR of *VIN3* and *ADH1* in Col-0 and *prt6-1* under normoxia (21% O_2) or following 24h hypoxia (1% O_2) treatment. Data are average of 3 biological replicates. **(h)** In vitro cycloheximide (CHX) chase timecourse of VRN2-HA co-expressed with VIN3-HA, or co-incubated with the proteasome inhibitor bortezomib in the absence of VIN3-HA. **(i)** Steady state levels of VRN2-FLAG and FIE in *pVRN2::VRN2-FLAG* lines expressing an β-estradiol-inducible VIN3 construct (*pER8::VIN3*). Two independent lines treated with or without β-estradiol are shown, and RT-PCR shows relative levels of *VIN3*, *VRN2* and *ACTIN2* expression.

Figure 5: The PRT6 N-degron pathway confines VRN2 to discrete root tissues and negatively regulates root growth. (a) Histochemical GUS staining of 7-day old roots in Col-0 and *prt6-1* seedlings expressing WT or mutant (Ala2) *pVRN2::VRN2-GUS:* (i), primary root (PR) tip, scale bar = 1mm; ii lateral root primordium (LRP), scale bar = 500μm; iii, emerged LR. **(b)** Quantitative RT-PCR (qPCR) of VRN2 in different regions of WT or *prt6-1* primary roots. The Tip and Main regions are shown in (a). Data are average of 3 biological replicates. **(c)** Representative images of 10 day old WT and mutant seedling roots in the Col-0 background. Scale bar = 1cm. **(d)** Quantified PR lengths and **(e)** emerged LR densities of 10 day old Col-0 WT and mutant lines (n=13-24). **(f)** Representative images of 6 day old Col-0 and *vrn2*-5 primary root meristems stained with propidium iodide. Asterix = quiescent centre; arrow head indicates end of meristem. Scale bar = 100μm. **(g)** Quantification of meristem size in Col-0 and *vrn2-5*. Data calculated from confocal root images (n=10). Box and whiskers plots show max and min, 25th to 75th percentiles, median and mean (+). Letters indicate one way ANOVA; Tukey's test ($p<0.05$-0.01).

Figure 6: Ectopic stabilisation of VRN2 enhances its negative effects on root system architecture. (a) Representative images of 10 day old *vrn2-1 fca-1*, *pVRN2::VRN2-GUS* and *pVRN2::Ala-VRN2-GUS* lines. Scale bar =1cm **(c)** Quantified PR lengths and **(c)** emerged LR densities for *vrn2-1 fca-1*, and *vrn2-1 fca-1* transformed with *pVRN2::VRN2-GUS* or *pVRN2::Ala-VRN2-GUS* lines (n=15-18). Box and whiskers plots show max and min, 25th to 75th percentiles, median and mean (+). Letters indicate one way ANOVA; Tukey's test ($p<0.05$-0.01).

Supporting information

Figure S1. Genotyping PCR confirming homozygosity of mutants in the Col-0 FRI-Sf2 background

Table S1. Primer sequences used in this study

Figure 1

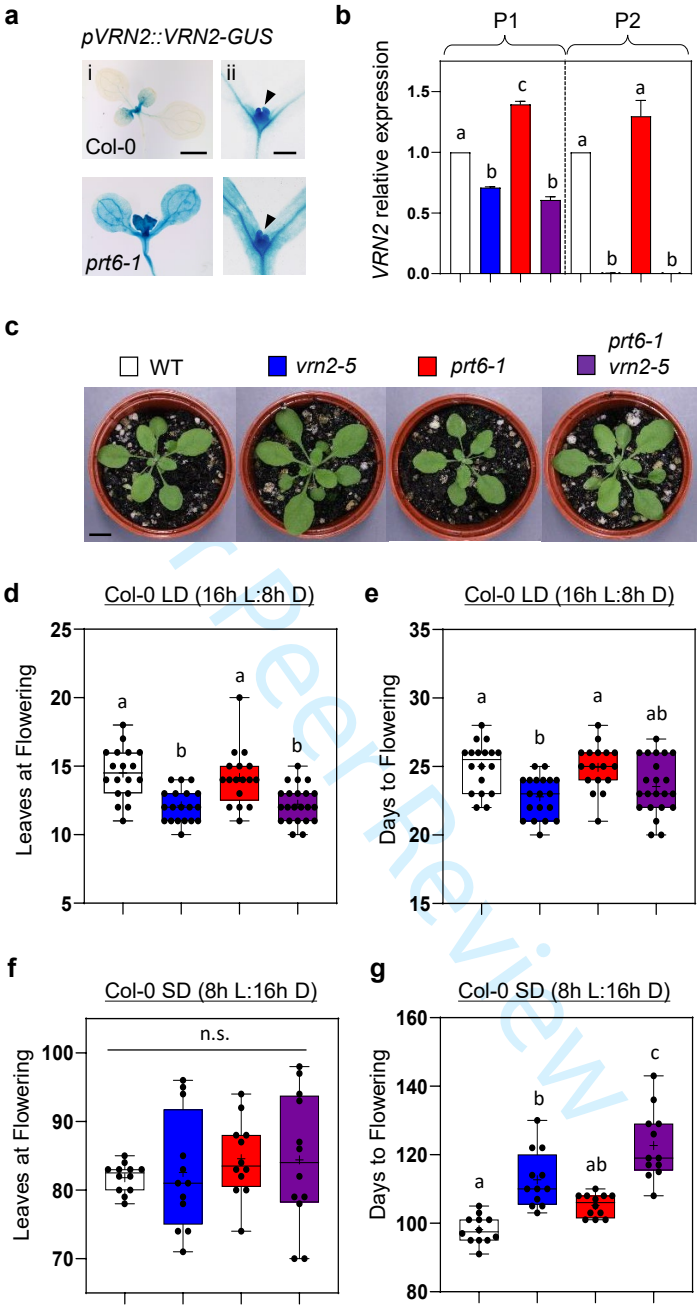

Figure 2

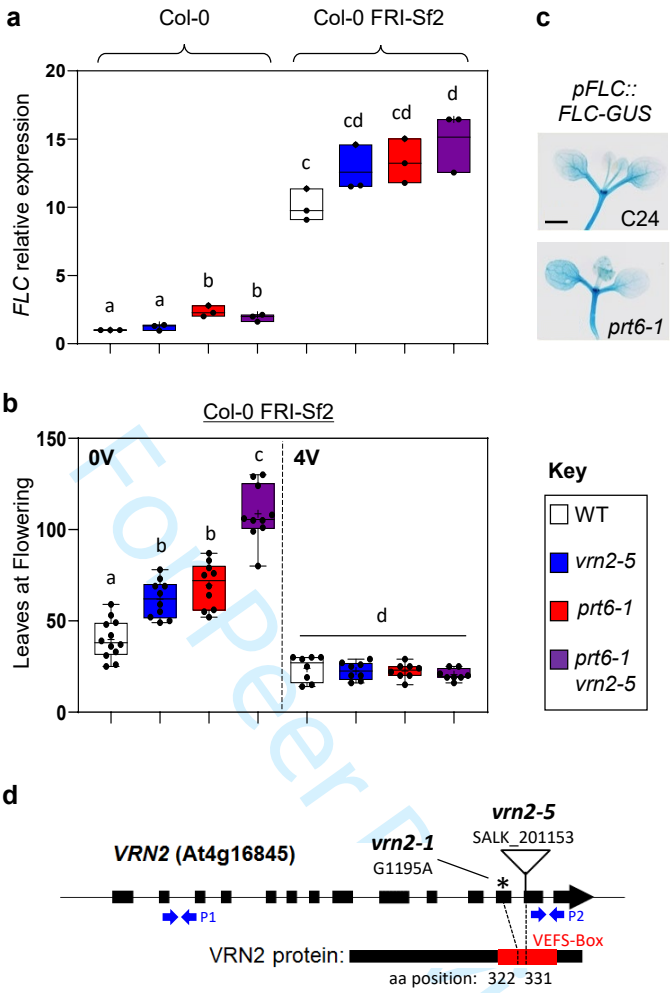

Figure 3

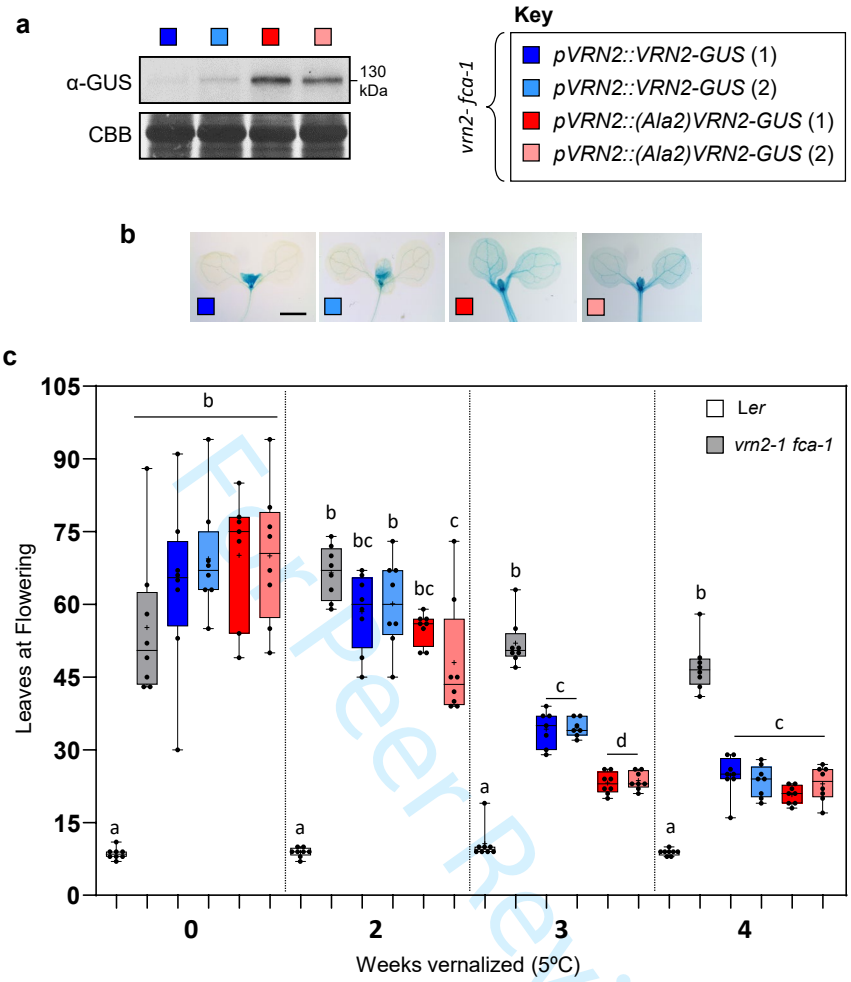

Figure 4

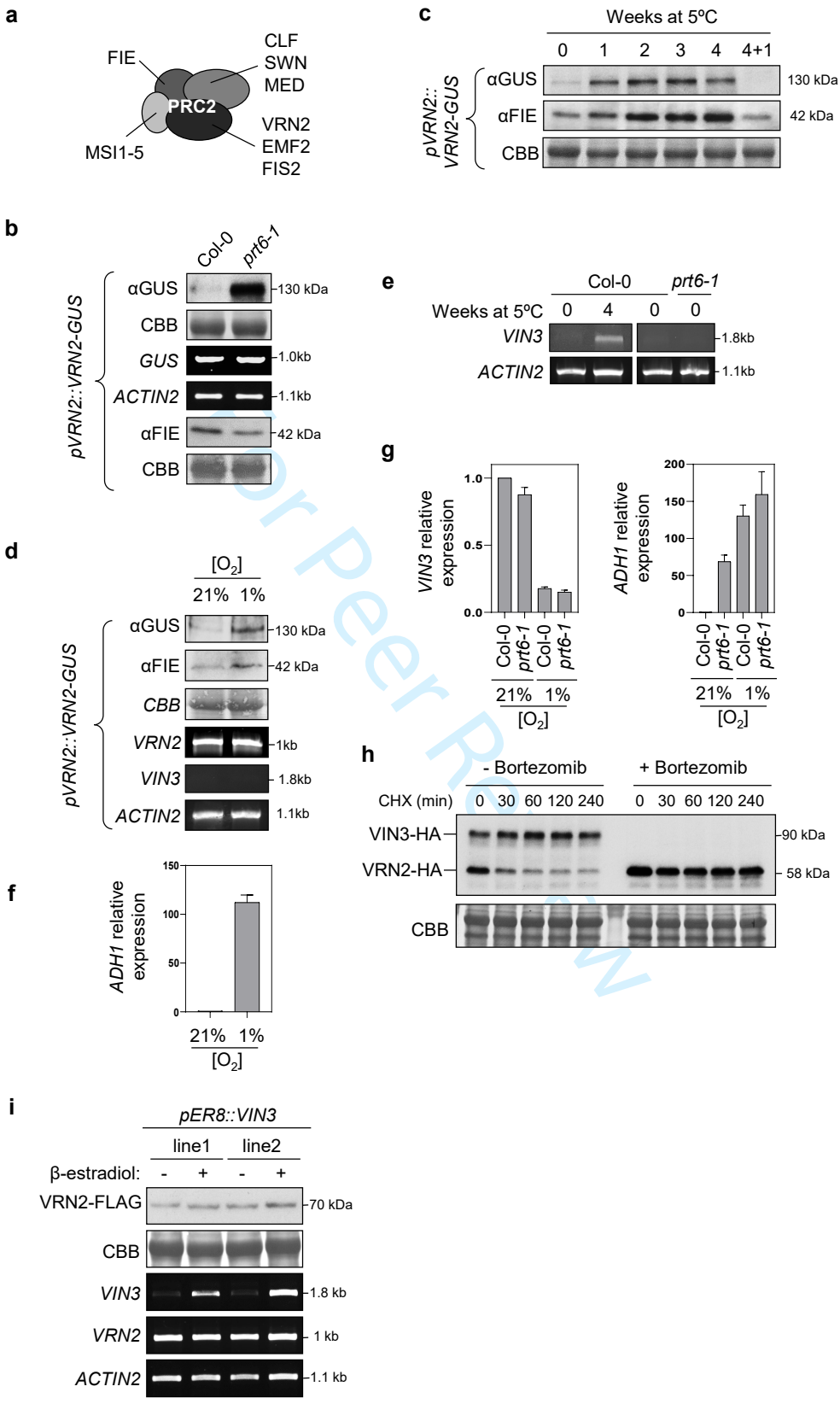

Figure 5

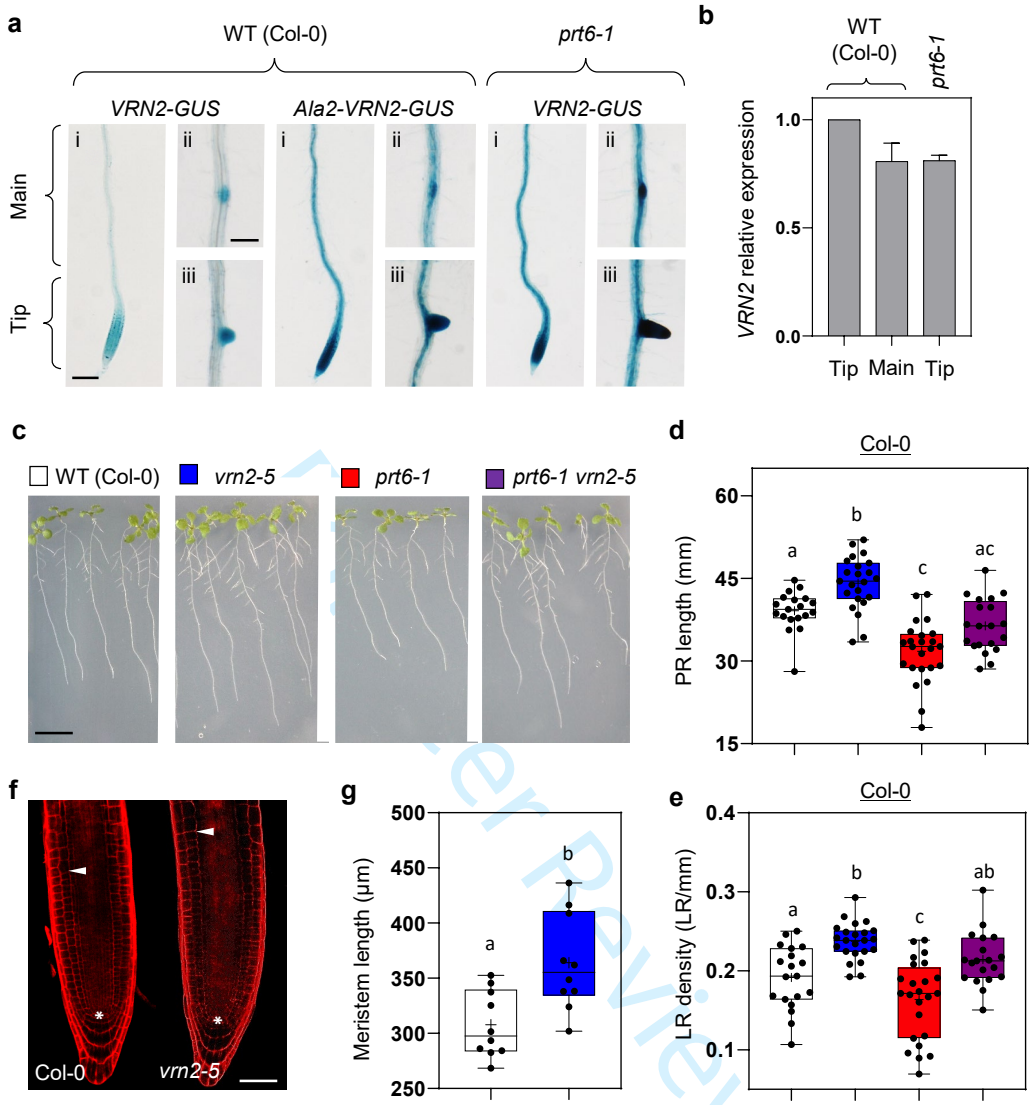

Figure 6